

A METHOD FOR GEOMETRIC PROCESSING OF OPTICAL SATELLITE IMAGES USING AUTOMATICALLY DETERMINED GROUND CONTROL INFORMATION

Rupert Müller*, Thomas Krauß, Mathias Schneider, Peter Reinartz

German Aerospace Centre (DLR)
Remote Sensing Technology Institute
82234 Weßling, Germany

Commission I, WG I/5

KEY WORDS: Orthorectification, Direct Georeferencing, RPC, Image Matching, Processing Chain

ABSTRACT:

Orthorectification is the process to convert imagery into map-accurate forms by removing sensor, satellite motion and terrain related geometric distortions from raw imagery and is one of the main pre-processing steps for application oriented evaluations. Although optical satellite data of high geometric resolution can be orthorectified to absolute geometric accuracies of about 5 m to several hundred meters - depending on the satellite mission - using the metadata information from the satellite data providers (e.g. satellite position, velocity and attitude at any instant of time during data acquisition, camera internal geometry), there is still a need to improve the geometric accuracy by using Ground Control Points (three dimensional real world coordinates, which have to be identified in the satellite image). The manual measurement of such Ground Control Points by operators is a time consuming work leading to a cost and time ineffective project completion. This paper proposes a method and procedure to automatically extract Ground Control Points from already existing orthorectified images of superior geometric quality (reference images), which are used to improve the geometric accuracy as well as to produce at least consistent data sets.

1. INTRODUCTION

The geometric correction of remotely sensed image data is one of the key issues in multi-source data integration and is one of the main processing steps prior to further evaluation of the image data – namely fusion and analysis with data from different sources and times, overlaying with existing data sets or maps, change detection, map updating or integration into Geographic Information Systems (GIS). Although optical satellite data of high (and very high) geometric resolution can be orthorectified without the use of Ground Control Points (GCP) to absolute geometric accuracies of about 5 m to several hundred meters, depending on the satellite mission, there is still a need to improve the geometric accuracy by using GCP. The manual measurement of GCP is a time consuming work leading to a cost and time ineffective project completion. An automatic and operational processing chain to orthorectify high resolution optical satellite data (up to 5-10 m ground sampling distance) is proposed, which uses a (global) reference data base to extract GCP.

In the first processing step tie points between the optical image data and the reference image data are determined using a hierarchical image intensity based matching technique. Based on these tie points a GCP set is constructed. In the second processing step improved sensor model parameters are estimated from GCP information by least squares adjustment. A rigorous sensor model as used in Direct Georeferencing techniques and a universal sensor model as used in Rational Polynomial Functions are the basis for the adjustment process. In the third processing step the improved sensor models are applied to orthorectify the image underlying the height information from a DEM and to derive geometric quality

information like Root Mean Square Errors (RMSE) or residual plots.

On behalf of the European Space Agency (ESA) the geometric processing chain has been successfully applied for different projects – namely the UrbanAtlas and Image2006 project - using SPOT 4 HRVIR, SPOT 5 HRG, IRS-P6 LISS III and ALOS AVNIR-2 optical sensor data.

2. METHODOLOGY

2.1 Orthorectification

For the geometric processing of remotely sensed images from optical instruments mainly two approaches are in common use: First rigorous sensor models as used in Direct Georeferencing (DG) techniques, which describe physically the image generation process from the focal plane location of an instrument pixel to an earth surface location in terms of earth bound coordinate frames, and second the Rational Polynomial Function (RPF) model, which provide a standardized and easy to use mathematical model to map object coordinates to image column and row values of the original image. In this context the RPF model is derived from an already existing rigorous sensor model. Detailed descriptions on sensor models can be found in (Jacobsen, K. 2008, Poli, D. 2005 and Toutin, T. 2004).

Direct Georeferencing

The basic formula for the DG model is the collinearity equation, which relates the coordinates of an object point $\mathbf{r}_{object}^{earth}$, expressed in an earth bound mapping coordinate frame, to the image coordinate $\mathbf{r}_{object}^{sensor}$ of the same object point,

* rupert.mueller@dlr.de

which is derived from the measured pixel position in the sensor's coordinate frame. The rigorous relationship between 2D image coordinates and 3D object coordinates is given by

$$\mathbf{r}_{object}^{earth} = \mathbf{r}_{sensor}^{earth} + \mathbf{s} \cdot \mathbf{R}_{body}^{earth} \cdot \mathbf{R}_{sensor}^{body} \cdot \mathbf{r}_{object}^{sensor} \quad (1)$$

where $\mathbf{R}_{sensor}^{body}$ denotes the rotation around the three angles $(\varepsilon_x, \varepsilon_y, \varepsilon_z)$ from the sensor to the body coordinate frame, also referred to as boresight alignment angles or instrument mounting angles, and $\mathbf{R}_{body}^{earth}$ denotes the rotation around the angles $(\omega, \varphi, \kappa)$ from the body to a earth coordinate frame, which is derived from the angular measurements. This rigorous physical model utilizes on-board measurements from Star Tracker Systems (STS), Inertial Measurement Units (IMU), Global Navigation Systems (GNS) as well as the geometric sensor characterisation by laboratory and/or in-flight calibration. Considering high precision position determination of satellite systems (increasingly sub-meter range position accuracies become state-of-the art) as well as stable interior orientation of camera systems the improvement of satellite attitude / sensor alignment angles using GCP is one of the major tasks. Especially thermal effects caused by the sun exposure time during satellite orbit revolution influences the relative alignment between the body and the sensor coordinate frames and leads to pointing errors. A thermal stable connection between the camera system and the attitude measurement system like star trackers as well as a compact assembly with close distances between the devices is often hard to establish, which results in a thermal sensitive behaviour. For example such thermal influences are described and modelled for the SPOT 5 HRS sensor using a latitudinal model (Bouillon et al. 2003) or for the ALOS / PRISM sensor using a orbit cycle short term model (Takaku et al. 2007 and JAXA 2006). Therefore by iterative least squares adjustment improved alignment angles $(\varepsilon_x, \varepsilon_y, \varepsilon_z)$ are estimated and introduced in the physical sensor model (Müller et al. 2005). The improved sensor model is finally applied to orthorectify the optical data by object point reconstruction using interpolated terrain height values from the DEM and by transformation of planar object points to a map projection including appropriate pixel value resampling within a regular grid.

Rational Polynomial Function

Exterior and interior orientation can be implicitly encoded in form of rational polynomial functions (RPF) using third order polynomials for nominator and denominator (80 coefficients). This Universal Sensor Model (USM) provides the transformation of object space coordinates to image space coordinates, which is available in standard format for a lot of remote sensing satellite systems. Each of the RPF for row and column is given via a ratio of 2 polynomials of third order in normalized λ , φ , and h with 20 coefficients.

$$\begin{aligned} r &= rpf_r(\lambda, \varphi, h) \\ c &= rpf_c(\lambda, \varphi, h) \end{aligned} \quad (2)$$

where r , c are row and column coordinates of the image and λ , φ , and h are longitude, latitude and ellipsoidal height in geographic coordinates of WGS84 datum. The coefficients used in the RPF are derived from the rigorous sensor model and

therefore the geometric accuracy of orthorectification is less or equal to the results received from the rigorous sensor model.

In order to improve the geometric accuracy of the original RPC these have to be corrected via ground control information. An affine transformation is estimated by least squares adjustment via the GCP. The corrected image coordinates are calculated based on this affine transformation and the RPF given by

$$\begin{aligned} row &= a_0 + a_1 \cdot rpf_r + a_2 \cdot rpf_c \\ col &= b_0 + b_1 \cdot rpf_r + b_2 \cdot rpf_c \end{aligned} \quad (3)$$

where rpf_r and rpf_c are the originally provided rational polynomial functions (Lehner et al., 2005).

2.2 Processing Chain

The mentioned sensor models lead (often) to good results in terms of absolute geometric accuracy, but nevertheless by introducing GCP information the geometric accuracy can be significantly improved. Figure 1 illustrates the processing chain to improve the geometric accuracy of the orthorectification by automatically derived GCP from reference images (already orthorectified scenes of superior geometric quality).

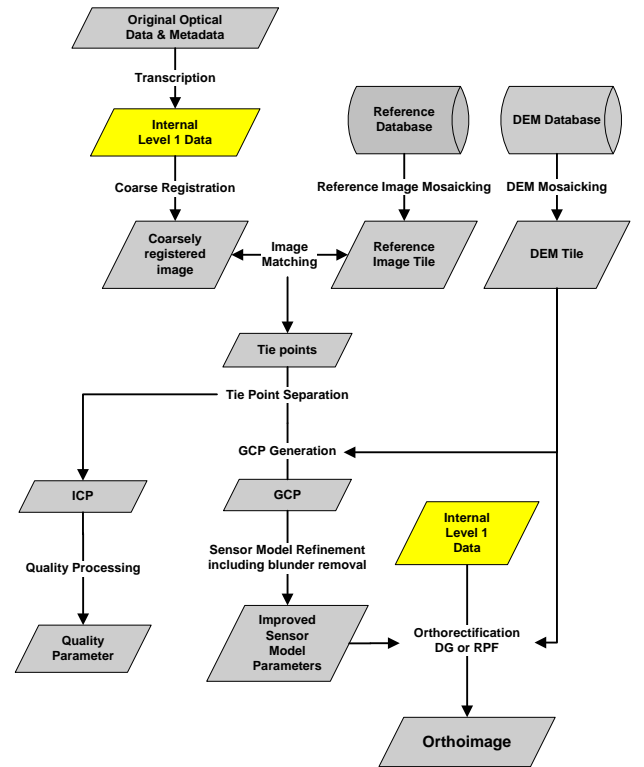


Figure 1 Processing Chain

The processing steps are:

- **Transcription:** The transcription system reformats the original image to an internal image format. The metadata needed for further processing are extracted and pre-processed in a following way that the processor system can handle the metadata information. This part of the processing chain is the only one, which has to be adopted for each sensor system.
- **Reference Image & DEM Mosaicking:** The (coarse) image corner coordinates, coming with the original data product, determine the region to extract congruent tiles

from the DEM database and from the reference image database. The image tiles are mosaicked with a margin of about 2 km due to the pointing knowledge of the sensor system.

- Coarse Registration:** Again based on the four image corner coordinates a coarse image registration of the internal level 1 original data is performed using a simple geometric affine transformation (most image matching techniques require a coarse geometric similarity of the matching partners). The coarse registered images are the starting point for the image matching with the reference image tiles. This step also includes the extraction and merging of image channels (e.g. generation of a panchromatic image) corresponding to the characteristics of the reference images in order to achieve good matching results.
- Image Matching:** In order to automatically extract GCP/ICP (Ground Control Points / Independent Control Points) from the reference image a hierarchical intensity based matching is performed (Lehner et al. 1992, Kornus et al. 2000). The matching process uses a resolution pyramid to cope with large image differences between the reference and the coarse orthorectified image. Based on the Forstner interest operator pattern windows are selected in one of the images and located with an accuracy of about one pixel in the other image via the maximum of the normalized correlation coefficients computed by sliding the pattern area all over the search area. The search areas in the matching partner image are determined by estimation of local affine transformations based on already available tie points in the neighborhood (normally from a coarser level of the image pyramid). The approximate tie point coordinates are then refined to sub-pixel accuracy by local least squares matching. The number of points found and their final (sub-pixel) accuracy achieved depend mainly on image similarity and decrease with time gaps between imaging. Only points with high correlation and quality figure are selected as tie points including cross checking by backward matching of all found points. It is noted that other matching techniques and reference data types are possible than the above mentioned intensity based image matching. For example the shaded DEM matching technique (Schneider et al. 2009) or a multimodal image matching method based on similarity metrics like Mutual Information using SAR reference images (Reinartz et al. 2010). A weighted combination of the results from different matching techniques is a promising outlook to improve and to stabilize the automatic GCP generation.
- Tie Point Separation & GCP Generation:** The set of tie points is subdivided into GCP candidates used for the improvement of the sensor models and an ICP set used for geometric quality assessment. The selection of GCP is based on the requirement of equally distributed points over the scene with high quality figure. In order generate fully qualified three dimensional GCP the selected tie points are supplemented by bilinear interpolated DEM values extracted from the DEM tile.
- Sensor Model Refinement & Blunder Detection:** As mentioned in chapter 2.1 improved sensor model parameters are estimated based on the GCP information. For DG the alignment angles are refined and for RPF the affine transformation parameters are estimated. Within the Least Squares Adjustment iterative blunder detection is integrated, which eliminates step by step GCP with a

residual greater than a threshold (e.g. 2 pixels) starting with the lowest quality GCP (see also chapter 2.3).

- Orthorectification:** Finally the original scene is orthorectified using the improved sensor model parameters and the DEM to account for terrain displacements as described in chapter 2.1.
- Quality Processing:** The tie points of less quality serve as independent control points (ICP) to derive automatically a quality record (RMSE values, residual plots).

2.3 Blunder Detection

Within the automatic and operational processing chain blunder detection is of high significance. Different levels of blunder detection are included to determine a reliable set of GCP with high geometric quality. As mentioned before, only points with good registration consistency (high correlation and quality figure) are selected based on threshold values. A further method for blunder detection is integrated in the least squares adjustment, which eliminates iteratively GCP with a residual greater than a threshold starting with the lowest quality GCP. In this context a residual is defined as deviation of GCP coordinates from the re-calculated object point coordinates using the refined sensor model, which has been derived from the adjustment using all currently valid GCP. In a first step the whole GCP set serves as input for the iterative parameter estimation. Successively the GCP with lowest quality and residuals greater than a threshold is removed from the GCP set. This iterative procedure is repeated until a GCP set remains, which is consistent to the sensor model. The procedure has to be iterative, because each GCP influences the result of the parameter estimation.

The determination of the GCP blunder detection threshold is exemplarily shown for an image scene acquired by the SPOT 4 HRVIR instrument. Figure 2 shows the histogram of the residuals (2-dimensional $RMSE_{xy}$) after the sensor model refinement by least squares adjustment: In the first case using the initial GCP set (before blunder removal) and in the second case using a subset of GCP (after the blunder removal).

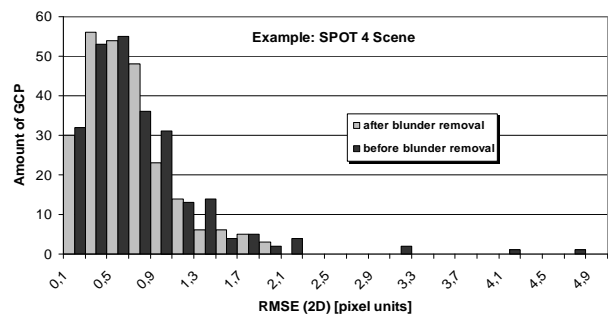


Figure 2 Histogram of the residuals ($RMSE_{xy}$) after least squares adjustment for one SPOT 4 HRVIR scene. Dark bars: before blunder removal; bright bars: after blunder removal using 2 pixel sizes as GCP rejection level.

For the blunder detection threshold two pixel sizes is assumed. This threshold separates outliers from good GCP as can be derived from Figure 2. A statistical evaluation of all scenes confirms this choice. The improvement in terms of the $RMSE_{xy}$ value at the GCP is 0.3 pixels (RMSE decreases from 1.0 pixel to 0.7 pixels) for this scene.

The drawback of this method is that systematic errors for the majority of the GCP can lead to erroneous or shifted values of the estimated parameters. Another possible error source is

obtained by a poor distribution of the GCP concentrated in only one part of the scene and a model estimated from such a distribution might not be ideal and consistent for the entire scene.

3. RESULTS

On behalf of the European Space Agency (ESA) the geometric processing chain has been applied for different projects – namely the UrbanAtlas and Image2006 project - using SPOT 4 HRVIR, SPOT 5 HRG*, IRS-P6 LISS III† and ALOS AVNIR-2 optical sensor data.

3.1 Image2006

The GMES (Global Monitoring for Environment and Security) Fast Track Land monitoring Service (FTLS) is a service to provide on a regular basis land cover and land use change datasets, which can be used by a wide range of downstream services at European, national, regional and local scale. Under ESA contract DLR (German Aerospace Center) produced two multi-temporal datasets of orthorectified images covering the participating EU27 and neighbouring countries (overall 38 countries). Two complete European coverages consisting of about 3700 scenes have been processed for the reference year 2006 (+/- 1 year) (referred to as Image2006). The orthorectified products are derived from a mixture of high resolution satellite images from SPOT 4 HRVIR with 20 m GSD, SPOT 5 HRG with 10 m GSD and IRS-P6 LISS III with 23 m GSD, each with

RMSE_y). For all other countries the USGS ETM+ Land Cover dataset given in UTM projection with a resolution of 28.5 m and a global accuracy of about 50 m RMSE_{xy} serves as absolute reference. It is noted that the geometric accuracy of the USGS ETM+ Land Cover dataset is for the European area is better than the official RMSE value, which is related on a global scale.

The DEM database is derived from SRTM-C band Version 2 of NASA and improved by using inputs from MONAPRO, GLOBE and SRTM-X band DEM within a fusion process. Parts of the DEM dataset are manually edited to remove blunder areas. The DEM is given in geographic projection (geodetic datum WGS84) with 1 arcsec planar resolution (~30 m) with ellipsoid heights. The height accuracy (1σ) of the DEM is about 6m in flat areas and up to 30 m in mountainous areas. In the Alps greater parts of MONAPRO and in east Turkey greater parts of GLOBE has to be used (Roth et al. 2002).

Relative Geometric Accuracy

Figure 3 shows the results broken down into the processed countries and the two coverages. The first two columns of each country show the RMS errors in x (east) and y (north) direction for the first coverage. The last two columns are valid for the second coverage. For SPOT4/5 and IRS-P6 orthorectified scenes an overall geometric accuracy with respect to the reference images (relative error) of about 10 m RMSE in each direction (RMSE_{xy}=13.2 m) is reached (for Spot4/5: RMSE_x=10.4 m, RMSE_y=8.6 m, RMSE_{xy}=13.6 and for IRSP6:

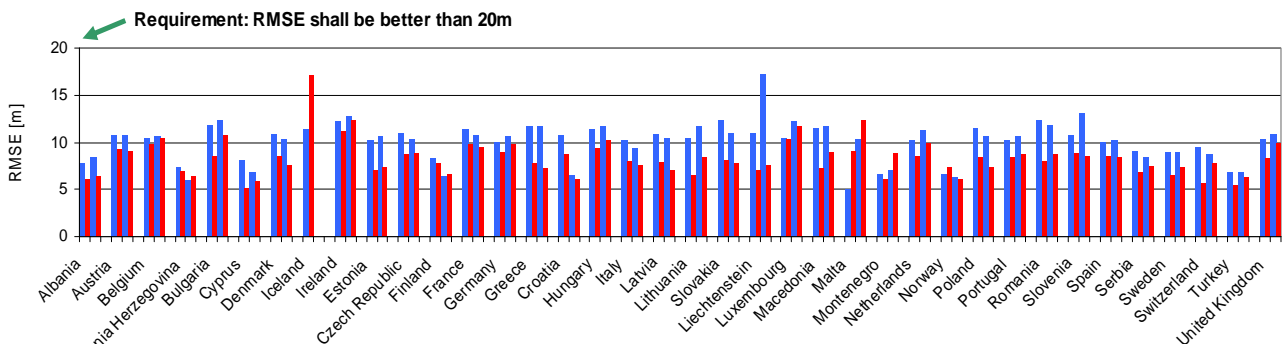


Figure 3 Geometric accuracy (RMSE) of Image2006 products w.r.t. reference images (relative accuracy). RMSE_x (blue) and RMSE_y (red) for European coverage 1 (first two columns of country) and European coverage 2 (last two columns of country)

four spectral bands. About 95 % of the images could be automatically processed (Müller et al. 2008),

For the countries, which took part in the IMAGE2000‡ project, the reference images are the orthorectified panchromatic images derived from Landsat 7 Enhanced Thematic Mapper ETM+ imagery given in geographic projection with a resolution of 0.000115° and an accuracy of about 9-15 m RMSE_x and 7-18 m RMSE_y (except for Austria with about 52 m RMSE_x and 27 m

RMSE_x=9.7 m, RMSE_y=8.0 m, RMSE_{xy}=12.6), which corresponds to half a pixel size. It has to be considered that for Spot, unlike for IRSP6, an oblique view up to 30° is possible, so that DEM errors influence the geometric accuracy of the orthoimages generated from Spot. The mean number of ICP used for the quality assessment is 5496 points per scene for IRS-P6 and 1360 points per scene for SPOT 4/5, which is an average of about 450 ICP per 1000 km².

Absolute Geometric Accuracy

The absolute accuracy has been manually derived by different operators using maps of scale 1:10.000 to 1:50.000 and aerial orthophotos for different areas in Europe. The RMSE values at these selected areas are shown in Table 1. The absolute geometric accuracy is of same magnitude as the relative geometric accuracy. The reason for this has to be investigated in more detail.

* © CNES 2007 Distribution Spot Image S.A., France, all rights reserved; produced by DLR/Metria – data provided under an ESA contract for FTS LM IMAGE2006

† © ANTRIX Corporation Limited 2007, Distribution by Euromap GmbH, Germany, all rights reserved; produced by DLR/Metria - data provided under an ESA contract for FTS LM IMAGE2006

‡ © European Communities, Source: Joint Research Centre IMAGE2000, based on Landsat 7 ETM+ © ESA, distributed by Eurimage; ortho-correction EU15 © Metria, ortho-correction other countries GISAT; mosaic production GISAT

Table 1 Absolute geometric accuracy values derived by manually measured GCP at selected areas in Europe.

Area	RMSE _x [m]	RMSE _y [m]	N
Paris / France	6.7	9.1	30
Montpellier / France	11.5	7.6	20
Prag / Czech Rep.	10.3	7.4	20
Rom / Italy	9.9	10.5	17
Milano / Italy	8.6	11.5	14
Rzeszow / Poland	19.5	13.1	17
Marseille / France	7.8	9.4	17
Wessling / Germany	6.3	5.6	34

3.2 UrbanAtlas

The GMES Land Information Service Urban Atlas provides detailed knowledge of urban land use, which is essential for monitoring and analyzing changes on a geolocated basis. Amongst other Earth Observation data the ALOS AVNIR-2 serve as input to compile major European cities and larger urban zones. The 4-channel multispectral instrument AVNIR-2 has a spatial resolution of 10 m with a across track pointing capability of 44°.

As reference image database the previously described Image2006 served as input. The relative geometric accuracy assessment is again based on the automatic extracted ICP. The number of extracted ICP varies for each image between 26 and 27515 with a mean number of approximately 5000 ICP per AVNIR-2 scene.

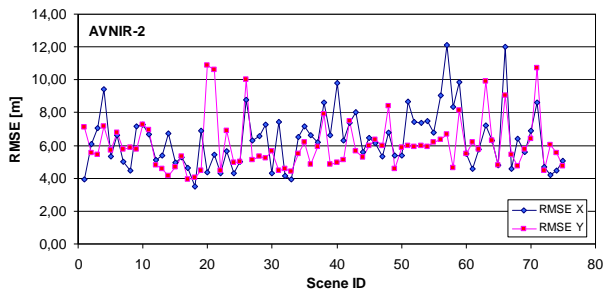


Figure 4 Geometric accuracy (RMSE) of ALOS AVNIR-2 orthorectified scenes w.r.t. reference images (relative accuracy). RMSE_x (blue) and RMSE_y (red)

The RMSE values in X-direction are between 3.5 m and 12.1 m and in Y-direction between 3.9 m and 10.7 m. That means that the geometric accuracy of the orthorectified AVNIR-2 scenes with respect to the used reference is in the order of about one pixel or better.

4. CONCLUSION

A new operational and automatic processing chain to orthorectify high resolution optical satellite images is proposed. The applicability of this method to very high resolution images depends on the availability of appropriate reference images. The performance of the processing chain has been demonstrated using a huge amount of images from SPOT 4 HRVIR, SPOT 5 HRG, IRS-P6 LISS III and ALOS AVNIR-2. The proposed method will be further applied within the Ground Segment of the upcoming hyperspectral satellite mission EnMAP

(Environmental Mapping and Analysis Program) (Müller et al. 2010).

REFERENCES

- Bouillon, A., Breton, E., De Lussy, F., Gachet, R., 2003. *SPOT5 Geometric image quality*. Proceedings of IGARSS 2003 Symposium, Toulouse France, July 21-25, 2003
- Kornus, W., Lehner, M., Schroeder, M., 2000. *Geometric inflight calibration by block adjustment using MOMS-2P 3-line-imagery of three intersecting stereo-strips*, SFPT (Société Française de Photogrammétrie et Télédétection), Bulletin Nr. 159, pp. 42-54
- Jacobsen, K., 2008. *Geometric modelling of linear CCDs and panoramic imagers*. In: Li, Z.; Chen, J.; Baltasvias, E. (Hrsg.): *Advances in Photogrammetry, Remote Sensing and Spatial Information Science*. London: Taylor and Francis, 2008, p. 145-155
- JAXA, 2006. *ALOS Algorithm description (PRISM/AVNIR-2)*, NEC TOSHIBA Space System, 2006
- Lehner, M., Gill, R.S., 1992. *Semi-Automatic Derivation of Digital Elevation Models from Stereoscopic 3-Line Scanner Data*, IAPRS, Vol. 29, part B4, Commission IV, pp. 68-75, Washington, USA
- Lehner, M., Müller, R., Reinartz, P., 2005. *DSM and Orthoimages from QuickBird and Ikonos Data Using Rational Polynomial Functions*, Proceedings of "High Resolution Earth Imaging for Geospatial Information", May 17-20, Hannover, Germany
- Müller, R., Lehner, M., Reinartz, P., Schroeder, M., 2005. *Evaluation of Spaceborne and Airborne Line Scanner Images using a generic Ortho Image Processor*, Proceedings of ISPRS Hannover Workshop, High Resolution Earth Imaging for Geospatial Information, Germany, 17-20 May, VOL XXXVI, Part I/W3, 6p, (on CDROM).
- Müller, R., Krauß, T., Lehner, M., Reinartz, P., Schroeder, M., Hörsch, B., 2008: *GMES Fast Track Land Service 2006-2008 - Orthorectification of SPOT 4/5 and IRS-P6 LISS III Data*. In: ISPRS Congress Beijing 2008, 2008, Beijing.
- Müller, R., Bachmann, M., Makasy, C. De Miguel, A., Müller, A. Neumann, A., Palubinskas, G., Richter, R., Schneider, M., Storch, T., Walzel, T., Kaufmann, H., Guanter, L., Segl, K., Heege, T., Kiselev, V., 2010. *The Processing Chain and Cal/Val Operations of the Future Hyperspectral Satellite Mission EnMAP*. IEEE . 2010 IEEE Aerospace Conference , 6.-13. März 2010 , Big Sky, USA. ISBN 978-1-4244-3888-4. ISSN 1095-323X
- Poli, D., 2005. *Modelling of Spaceborne Linear Array Sensors*; Diss. ETH NO. 15894; Institut für Geodäsie und Photogrammetrie; ETH Zürich; ISBN 3-906467-50-3.
- Reinartz, P., Müller, R., Suri, S., Schwind, P., 2010, *Improving Geometric Accuracy of Optical VHR Satellite Data using TerrasAR-X Data*. IEEE . 2010 IEEE Aerospace Conference , 6.-13. März 2010 , Big Sky, USA. ISBN 978-1-4244-3888-4. ISSN 1095-323X

Roth, A., Knöpfle, W., Strunz, G., Lehner, M., Reinartz, P., 2002, *Towards a Global Elevation Product: Combination of Multi-Source Digital Elevation Models*, Symposium on Geospatial Theory, Processing and Applications, Ottawa, 2002

Schneider, M., Reinartz, P., 2009. *MATCHING OF HIGH RESOLUTION OPTICAL DATA TO A SHADED DEM*. In: Proceedings of the IEEE Geoscience and Remote Sensing Symposium 2009 (IGARSS). IEEE IGARSS 2009, 13.-17.07.2009, Cape Town, South Africa.

Schwind, P., Schneider, M., Palubinskas, G., Storch, T., Müller, R., Richter, R., 2009. *Processors for ALOS Optical Data: Deconvolution, DEM Generation, Orthorectification, and Atmospheric Correction*, IEEE Transactions on Geoscience and Remote Sensing, doi: 10.1109/TGRS.2009.2015941.

Takaku, J., Tadono, T., 2007. *PRISM geometric validation and DSM generation status*, ALOS PI Symposium 2007, JAXA, Japan, Dezember 2007.

Toutin, T., 2004. *Geometric Processing of Remote Sensing Images: Models, Algorithms and Methods*. International Journal of Remote Sensing, vol. 25, no. 10, pp. 1893-1924(32).